Available online at www.sciencedirect.com
SCIENCE DIRECT
Tetrahedron 62 (2006) 7274–7283
Tetrahedron

The role of terminal tyrosine residues in the formation of tripeptide nanotubes: a crystallographic insight

Sudipta Ray,[a] Michael G. B. Drew,[b] Apurba Kumar Das[a] and Arindam Banerjee[a,*]

[a]*Department of Biological Chemistry, Indian Association for the Cultivation of Science, Jadavpur, Kolkata 700 032, West Bengal, India*
[b]*School of Chemistry, The University of Reading, Whiteknights, Reading RG6 6AD, UK*

Received 20 February 2006; revised 24 April 2006; accepted 18 May 2006
Available online 9 June 2006

Abstract—Terminally protected acyclic tripeptides containing tyrosine residues at both termini self-assemble into nanotubes in crystals through various non-covalent interactions including intermolecular hydrogen bonds. The nanotube has an average internal diameter of 5 Å (0.5 nm) and the tubular ensemble is developed through the hydrogen-bonded phenolic-OH side chains of tyrosine (Tyr) residues [*Org. Lett.* **2004**, *6*, 4463]. We have synthesized and studied several tripeptides **3**–**6** to probe the role of tyrosine residues in nanotube structure formation. These peptides either have only one Tyr residue at N- or C-termini or they have one or two terminally located phenylalanine (Phe) residues. These tripeptides failed to form any kind of nanotubular structure in the solid state. Single crystal X-ray diffraction studies of these peptides **3**–**6** clearly demonstrate that substitution of any one of the terminal Tyr residues in the Boc-Tyr-X-Tyr-OMe (X=Val or Ile) sequence disrupts the formation of the nanotubular structure indicating that the presence of two terminally located Tyr residues is vital for nanotube formation.

1. Introduction

Organic nanotubular architectures[1] have applications in the field of materials science, nanotechnology, and artificial ion channel[2] systems. Peptide nanotubular systems find useful applications in biology and medical sciences. They can be used as glucose transporter[3] or as transmembrane ion channels[2] or even as potential antibiotics against drug resistant bacteria.[4] Ghadiri and co-workers have compellingly demonstrated that 24- and 30-membered ring forming *cyclo* α-peptides with an even number of alternating D and L amino acid residues stack in an antiparallel β-sheet-like arrangement to form a hydrogen-bonded nanotubular structure.[5] Interestingly, related cyclic peptides consisting exclusively of β-amino acid residues,[6] or with an alternating arrangement of α- and β-amino acids,[7] or of vinylogous δ-amino acids[8] can also form nanotubular structures. Many successful attempts have previously been made to create nanotubular structures using various self-assembling organic compounds including cyclic oligoureas,[9] cyclodextrin based polyionic amino acids,[10] 7-deaza-2-deoxy xanthosine dihydrate,[11] and others.[12] While the self-association of cyclic peptides or peptide derivatives into hollow nanotubes has been studied in detail, the formation of acyclic peptide based nanotubes has been paid relatively less attention, there being only a few examples.[13] A recent study demonstrates the formation of nanotubes using self-assembly of a dipeptide D-Phe–D-Phe and insertion of platinum nanoparticles inside the tubes.[13c] Other studies of acyclic peptide based nanotube formation include the self-assembly of a truncated variants of Alzheimer's Aβ-peptide residue 16–22 (CH_3CO-KLVFFAE-NH_2) into a nanotubular structure in aqueous

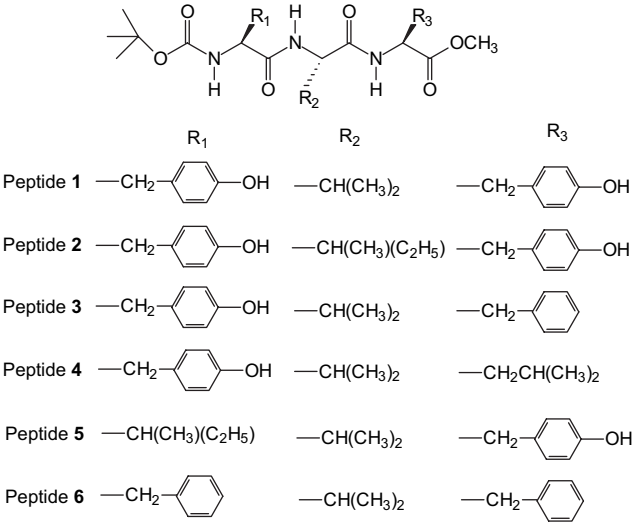

Figure 1. Schematic presentation of tripeptides **1**, **2**, **3**, **4**, **5**, and **6**.

Keywords: Acyclic peptides; Tyrosine; Nanotube; Self-assembly.
* Corresponding author. Tel.: +91 33 2473 4971; fax: +91 33 2473 2805; e-mail: bcab@mahendra.iacs.res.in

0040–4020/$ - see front matter © 2006 Elsevier Ltd. All rights reserved.
doi:10.1016/j.tet.2006.05.042

solution[13d] and the self-association of surfactant-like peptides with variable glycine tails into nanotubes of diameter 30–50 nm at neutral pH.[13e]

In our previous communication, we demonstrated that peptides **1** and **2**, each containing two terminal Tyr residues are able to form nanotubes in crystals. In this paper, we are addressing the question whether any change of the terminal Tyr residue can retain (or not) the nanotubular structure in crystals. Keeping this in mind, several tripeptides **3**–**6** (Boc-Tyr(1)-Val(2)-Phe(3)-OMe **3**, Boc-Tyr(1)-Val(2)-Leu(3)-OMe **4**, Boc-Ile(1)-Val(2)-Tyr(3)-OMe **5**, and Boc-Phe(1)-Val(2)-Phe(3)-OMe **6**) (Fig. 1) with only one terminally positioned tyrosine or no Tyr residue, have been synthesized, purified, characterized, and their self-assembling behavior in crystals have been studied in detail to probe whether any of these peptides are able to form nanotubular structures in the solid state.

2. Results and discussion

Single crystals suitable for X-ray diffraction of tripeptides **1**–**6** were obtained from methanol–water solution by slow evaporation. Tripeptides **1** and **2** contain tyrosine residues at both termini and adopt β-sheet-like conformation in the crystal state. The individual peptide subunits are stacked one over another, maintaining proper registry, and form an open ended tube having an average internal diameter of 5.0 Å (0.5 nm) including van der Waals' contacts along the crystallographic *b* axis. The top view of the supramolecular cylindrical ensembles of peptide **2** in ball and stick models (Fig. 2a) and space-filling models (Fig. 2b) show that the interior of the peptide supramolecular channel is hydrophilic (due to the presence of hydrogen-bonded CONH moieties and phenolic-OH groups of Tyr residues), while the exterior is hydrophobic as it is occupied by the valine and isoleucine side chains and the N-terminally protecting Boc groups.[13f]

Tripeptide **3** contains a tyrosine residue at the N-terminus whereas there is a phenylalanine residue at the C-terminus. For peptide **3** there are two molecules in the asymmetric unit and they are held together by van der Waals' forces. The ORTEP diagram of this peptide is given in Figure 3a. Backbone torsion angles of each conformer (A and B) of peptide **3** are mostly in the extended region of the Ramachandran diagram[14] (Table 1). Each conformer then self-assembles by three intermolecular hydrogen bonds to form a columnar structure (for conformer A, N3A–H3A···O2A 2.13 Å, 2.92 Å, 149°, N9A–H9A···O8A 1.99 Å, 2.79 Å, 150°, and N6A–H6A···O5A 2.01 Å, 2.87 Å, 165° and for conformer B, N3B–H3B···O2B 2.17 Å, 2.93 Å, 146°, N9B–H9B···O8B 2.05 Å, 2.92 Å, 175°, and N6B–H6B···O5B 2.06 Å, 2.93 Å, 170°) (Table 2) along the crystallographic *b* direction (Fig. 4a). This columnar structure on further aggregation using van der Waals' interactions along the crystallographic *a* axis formed a complex quaternary β-sheet structure (Fig. 4b).

Tripeptide **4** contains a tyrosine residue at the N-terminus whereas tripeptide **5** possesses a tyrosine residue at the C-terminus with a centrally located Val residue in each case. The molecular conformation of tripeptide **4** in the crystal state is illustrated in Figure 3b. Most of the torsion angles (ϕ_1 −137.0(3), ψ_1 118.4(3), ϕ_2 −120.0(3), ψ_2 111.4(3), and ϕ_3 −122.8(3)) of the constituent amino acids residues of the tripeptide **4** fall within the parallel β-sheet region of the Ramachandran plot[14] (Table 1). Hence, the tripeptide **4** adopts an extended backbone conformation, which self-assembles through three intermolecular hydrogen bonds (N3–H3···O2 2.27, 3.01 Å, 144°, N9–H9···O8 2.13 Å, 2.99 Å, 173°, and N6–H6···O5 2.13 Å, 2.99 Å, 172°) (Table 2) along the crystallographic *c* axis to form a columnar structure (Fig. 5a). These columnar structures of tripeptide **4** are further self-assembled into higher order supramolecular β-sheet structures through intermolecular hydrogen bonds (O48–H48···O16 1.97 Å, 2.78 Å, 168°) along the

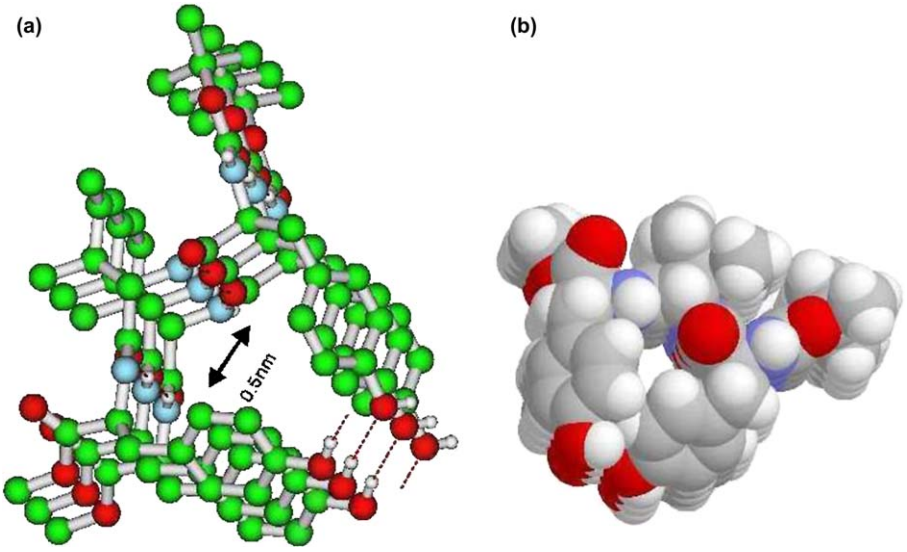

Figure 2. (a) Top view of the development of intermolecularly hydrogen-bonded nanotubular structure along the crystallographic *b* axis exhibiting internal tubular diameter of about 5.0 Å in ball and stick model. The tubular structure is composed of the acyclic peptide **2** subunit with extended backbone conformation (which adopts a β-strand like structure). (b) Space-filling model of the nanotubular ensemble obtained from a higher order self-assembly of the peptide **2**.

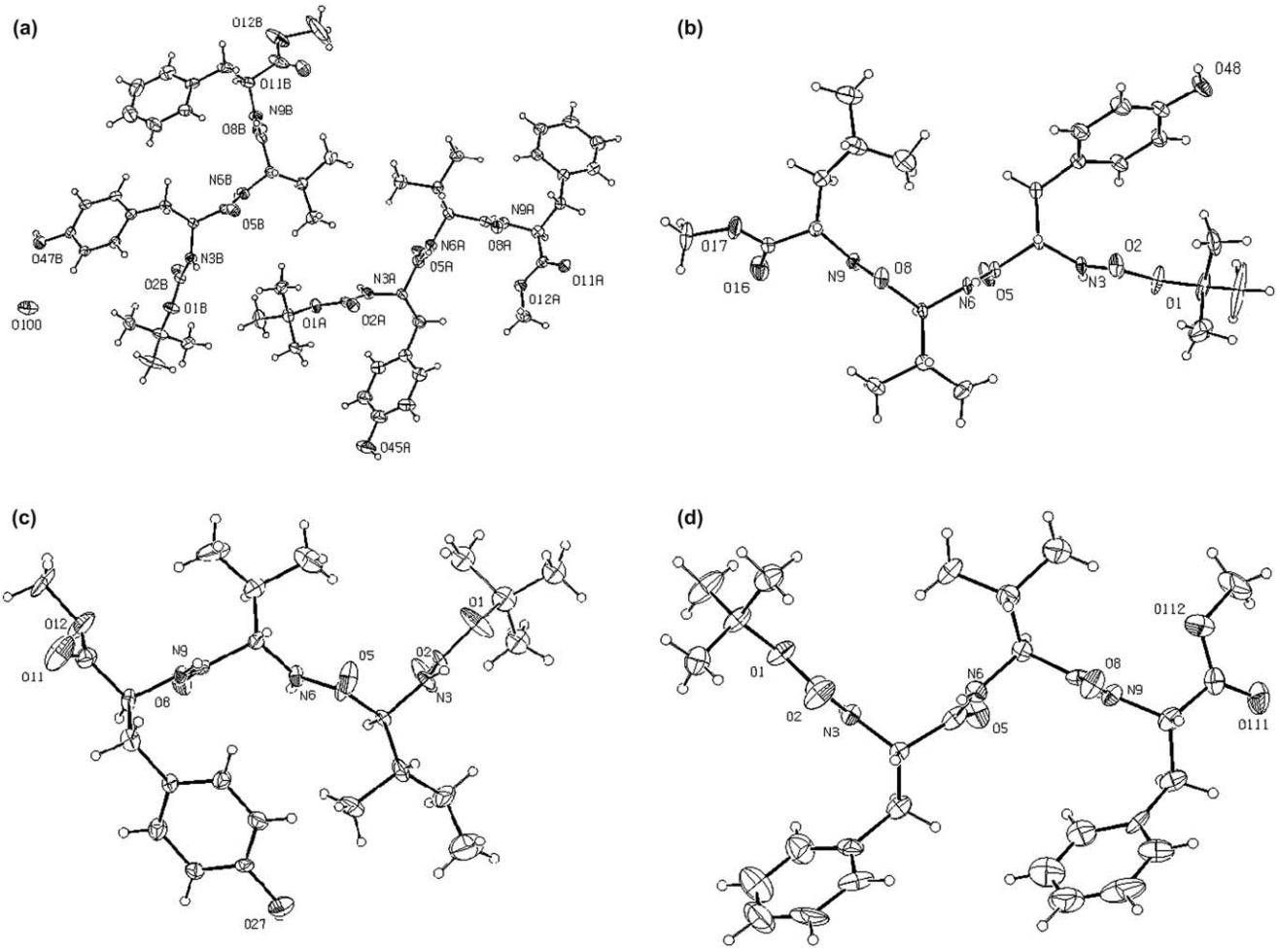

Figure 3. ORTEP diagrams with atomic numbering scheme for the (a) peptide **3**, (b) peptide **4**, (c) peptide **5**, and (d) peptide **6**. Thermal ellipsoids are shown at 30% probability level. Only nitrogen and oxygen atoms are labeled due to clarity.

crystallographic *a* direction and via van der Waals' interactions along the crystallographic *b* axis (Fig. 5b).

From the backbone torsion angles (ϕ_1 −116.6(8), ψ_1 110.6(7), ϕ_2 −124.5(7), ψ_2 119.8(7), and ϕ_3 −102.9(8)), it is clear that tripeptide **5** also adopts an extended backbone in its molecular structure. The molecular conformation of tripeptide **5** in the crystal state is illustrated in Figure 3c. Each subunit of tripeptide **5** self-assembles to form a columnar structure using three intermolecular hydrogen bonds (N3–H3···O2 2.08 Å, 2.94 Å, 173°, N9–H9···O8 2.05 Å, 2.91 Å, 173°, and N6–H6···O5 2.17 Å, 3.02 Å, 168°) (Table 2) along the crystallographic *b* axis (Fig. 6a). These columnar structures of tripeptide **5** are further self-assembled into higher order supramolecular structures using intermolecular hydrogen bonds (O27–H27···O27 2.08 Å, 2.85 Å, 157° with symmetry element $1-x$, $-1/2+y$, $-z$) involving the phenolic-OH groups of the Tyr residue, along the crystallographic *a* direction (Fig. 6b). Although tripeptides **4** and **5** contain one tyrosine residue at the C and N terminus, respectively, they are unable to form any nanotubular structure like peptides **1** and **2**.

The molecular conformation of the tripeptide **6** (Fig. 3d) was also established by a single crystal X-ray diffraction studies. Most of the ϕ and ψ values (ϕ_1 −103.5(6), ψ_1 97.8(6), ϕ_2 −102.1(7), ψ_2 97.8(7), and ϕ_3 −117.4(7)) with the exception of ψ_3 at 33.4(8) of the constituent amino acid residues of tripeptide **6** fall within the parallel β-sheet region of the Ramachandran plot and the peptide adopts an extended backbone structure. The individual peptide subunits self-assembles through intermolecular hydrogen bonds (N3–H3···O2 2.12 Å, 2.95 Å, 162°, N9–H9···O8 2.16 Å, 2.87 Å, 140°, and N6–H6···O5 2.12 Å, 2.97 Å, 167°) (Table 2) maintaining the proper registry to form a supramolecular columnar structure along the crystallographic *b* axis (Fig. 7a). Figure 7b clearly shows that peptide **6** also fails to form a nanotubular structure, instead it forms a complex sheet-like structure using van der Waals' interaction along the crystallographic *a* axis. Crystal data for peptides **3**, **4**, **5**, and **6** are listed in Table 3.

3. Conclusion

This study clearly demonstrates that there is a definite role of both terminally located Tyr residues for the formation of nanotubular structures. Any change in the terminally located Tyr residue by Phe or any other residues completely disrupts the crystal packing arrangement, which is

Table 1. Selected torsion angles (°) of peptides **3**, **4**, **5**, and **6**

Peptide **3**			
Molecule A			
O1A–C2A–N3A–C4A	−167.4(3) (ω_0)	N6A–C7A–C8A–N9A	104.4(4) (ψ_2)
C2A–N3A–C4A–C5A	−128.6(4) (ϕ_1)	C7A–C8A–N9A–C10A	−177.8(3) (ω_2)
N3A–C4A–C5A–N6A	115.0(4) (ψ_1)	C8A–N9A–C10A–C11A	48.6(4) (ϕ_3)
C4A–C5A–N6A–C7A	177.0(3) (ω_1)	N9A–C10A–C11A–O12A	45.2(4) (ψ_3)
C5A–N6A–C7A–C8A	−104.0(4) (ϕ_2)		
Molecule B			
O1B–C2B–N3B–C4B	−164.3(3) (ω_0)	N6B–C7B–C8B–N9B	108.0(4) (ψ_2)
C2B–N3B–C4B–C5B	−133.2(4) (ϕ_1)	C7B–C8B–N9B–C10B	178.3(4) (ω_2)
N3B–C4B–C5B–N6B	122.8(4) (ψ_1)	C8B–N9B–C10B–C11B	−87.8(5) (ϕ_3)
C4B–C5B–N6B–C7B	167.6(3) (ω_1)	N9B–C10B–C11B–O12B	146.1(5) (ψ_3)
C5B–N6B–C7B–C8B	−115.7(4) (ϕ_2)		
Peptide **4**			
O1–C2–N3–C4	17.5(5) (ω_0)	N6–C7–C8–N9	111.4(3) (ψ_2)
C2–N3–C4–C5	−137.0(3) (ϕ_1)	C7–C8–N9–C10	−174.4(3) (ω_2)
N3–C4–C5–N6	118.4(3) (ψ_1)	C8–N9–C10–C15	−122.8(3) (ϕ_3)
C4–C5–N6–C7	175.7(3) (ω_1)	N9–C10–C15–O16	−26.9(5) (ψ_3)
C5–N6–C7–C8	−120.0(3) (ϕ_2)		
Peptide **5**			
O1–C2–N3–C4	174.1(7) (ω_0)	N6–C7–C8–N9	119.8(7) (ψ_2)
C2–N3–C4–C5	−116.6(8) (ϕ_1)	C7–C8–N9–C10	179.7(7) (ω_2)
N3–C4–C5–N6	110.6(7) (ψ_1)	C8–N9–C10–C11	−102.9(8) (ϕ_3)
C4–C5–N6–C7	−168.1(7) (ω_1)	N9–C10–C11–O12	61.8(9) (ψ_3)
C5–N6–C7–C8	−124.5(7) (ϕ_2)		
Peptide **6**			
O1–C2–N3–C4	173.6(5) (ω_0)	N6–C7–C8–N9	97.8(7) (ψ_2)
C2–N3–C4–C5	−103.5(6) (ϕ_1)	C7–C8–N9–C10	175.8(6) (ω_2)
N3–C4–C5–N6	97.8(6) (ψ_1)	C8–N9–C10–C11	−117.4(7) (ϕ_3)
C4–C5–N6–C7	−169.0(5) (ω_1)	N9–C10–C11–O12	33.4(8) (ψ_3)
C5–N6–C7–C8	−102.1(7) (ϕ_2)		

necessary for nanotubular architecture formation. So, the presence of both the Tyr residues is essential for nanotubular structure formation as the phenolic-OH groups from these two terminally located Tyr residues are responsible for the construction of polar nanochannel-like structures. This study not only sheds some light on the future design and construction of acyclic peptide based nanotubular structure but also implies the active involvement of important functional residues in the formation and stability of the nanotubular structure.

Table 2. Intermolecular hydrogen bonding parameters of peptides **3**, **4**, **5**, and **6**

Peptides	D–H···A	H···A/Å	D···A/Å	D–H···A/°	Symmetry
Peptide **3**					
Molecule A	N3A–H3A···O2A	2.13	2.92	149	$x, -1+y, z$
	N6A–H6A···O5A	2.01	2.87	165	$x, 1+y, z$
	N9A–H9A···O8A	1.99	2.79	150	$x, -1+y, z$
Molecule B	N3B–H3B···O2B	2.17	2.93	146	$x, 1+y, z$
	N6B–H6B···O5B	2.06	2.93	170	$x, -1+y, z$
	N9B–H9B···O8B	2.05	2.92	175	$x, 1+y, z$
	O47B–H47C···O11A	1.91	2.71	160	$2-x, y, 2-z$
Peptide **4**					
	N3–H3···O2	2.27	3.01	144	$-1+x, y, z$
	N6–H6···O5	2.13	2.99	172	$1+x, y, z$
	N9–H9···O8	2.13	2.99	173	$-1+x, y, z$
	O48–H48···O16	1.97	2.78	168	$1+x, y, -1+z$
Peptide **5**					
	N3–H3···O2	2.08	2.94	173	$x, 1+y, z$
	N6–H6···O5	2.17	3.02	168	$x, -1+y, z$
	N9–H9···O8	2.05	2.91	173	$x, 1+y, z$
	O27–H27···O27	2.08	2.85	157	$1-x, -1/2+y, -z$
Peptide **6**					
	N3–H3···O2	2.12	2.95	162	$x, -1+y, z$
	N6–H6···O5	2.12	2.97	167	$x, 1+y, z$
	N9–H9···O8	2.16	2.87	140	$x, -1+y, z$

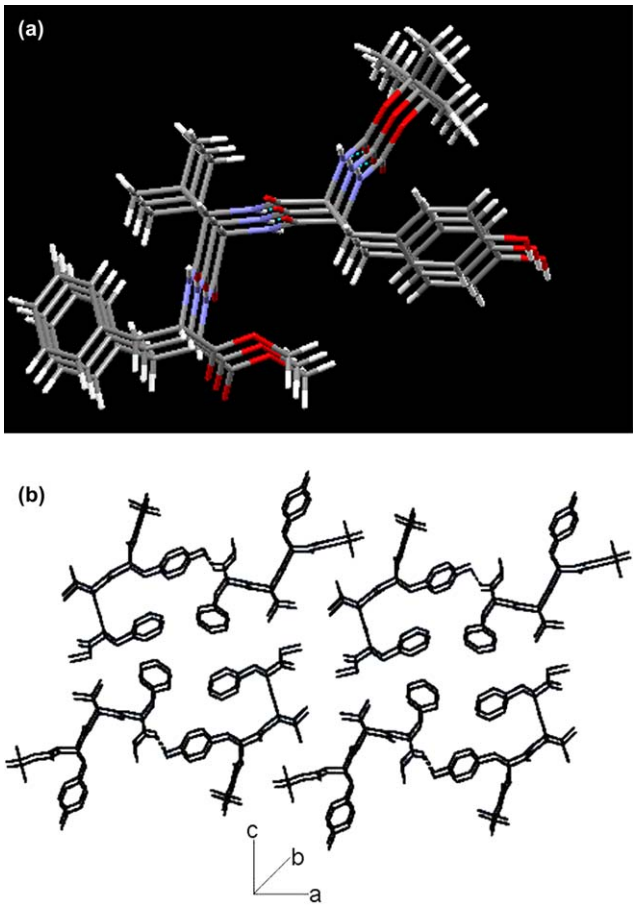

Figure 4. (a) Columnar packing of peptide **3** along crystallographic *b* direction and (b) packing diagram of the peptide **3** showing the formation of intermolecular hydrogen-bonded sheet-like structure along crystallographic *a* axis.

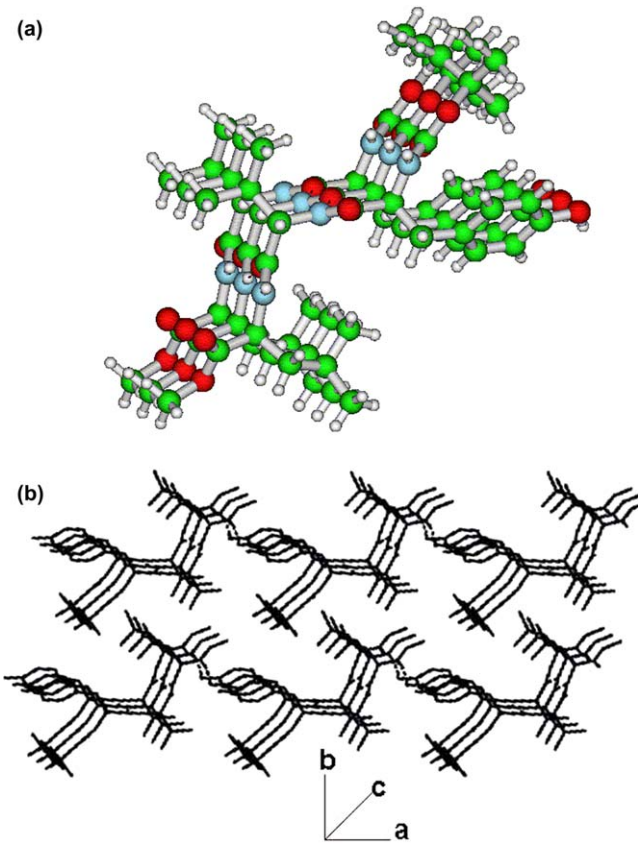

Figure 5. (a) Crystallographic view of a single molecule of peptide **4** along *c* axis. Nitrogen atoms are blue, oxygen atoms are red, carbon atoms are green, and hydrogen atoms are gray. Hydrogen bonds are shown as dotted lines. (b) Packing diagram of the peptide **4** showing the formation of intermolecular hydrogen-bonded complex sheet-like structure along crystallographic *a* axis.

4. Experimental

4.1. General

The tripeptides **1**, **2**, **3**, **4**, **5**, and **6** employed in this report have been synthesized by the conventional solution phase methodology.[15] The Boc group was used for N-terminal protection and the C-terminus was protected as a methyl ester. Couplings were mediated by di-cyclohexylcarbodiimide/1-hydroxybenzotriazole (DCC/HOBt). The final compounds were fully characterized by IR spectroscopy, ^{1}H NMR spectroscopy, and mass spectrometry.

4.2. Synthesis of peptide

4.2.1. Boc-Tyr(1)-OH 7. See Ref. 13f.

4.2.2. Boc-Tyr(1)-Val(2)-OMe 8. See Ref. 13f.

4.2.3. Boc-Tyr(1)-Val(2)-OH 9. See Ref. 13f.

4.2.4. Boc-Tyr(1)-Val(2)-Tyr(3)-OMe 1. See Ref. 13f.

4.2.5. Boc-Tyr(1)-Ile(2)-OMe 10. See Ref. 13f.

4.2.6. Boc-Tyr(1)-Ile(2)-OH 11. See Ref. 13f.

4.2.7. Boc-Tyr(1)-Ile(2)-Tyr(3)-OMe 2. See Ref. 13f.

4.2.8. Boc-Tyr(1)-Val(2)-Phe(3)-OMe 3. Boc-Tyr(1)-Val(2)-OH **9** (1.9 g, 5 mmol) in DMF (10 mL) was cooled in an ice-water bath. H-Phe-OMe was isolated from the corresponding methyl ester hydrochloride (2.15 g, 10 mmol) by neutralization, subsequent extraction with ethyl acetate and concentration to 10 mL, and it was added to the reaction mixture, followed immediately by DCC (1.03 g, 5 mmol) and HOBt (0.675 g, 5 mmol). The reaction mixture was stirred for three days. The reaction mixture was then taken in ethyl acetate (60 mL) and the DCU was filtered off. The organic layer was washed with 2 M HCl (3×50 mL), brine (2×50 mL), 1 M sodium carbonate (3×50 mL), and brine (2×50 mL) and then dried over anhydrous sodium sulfate and evaporated in vacuo to yield peptide **3** as a white solid. Purification was done by silica gel column (100–200 mesh) using 3:1 ethyl acetate/toluene as eluent.

Yield=2.16 g (4 mmol, 80%); R_f=0.66 (25% toluene/ethyl acetate); mp 70–72 °C; IR (KBr): 3324, 3293, 1714, 1691, 1647, 1521 cm^{-1}; $[\alpha]_D^{20}$ −20.3 (*c* 0.5, CH_3OH); ^{1}H NMR (300 MHz, $CDCl_3$) δ 7.10 (ring Hs of Tyr(1), 2H, d, *J*=6.6 Hz); 7.02 (ring Hs of Tyr(1), 2H, d, *J*=8.3 Hz); 6.74–6.71 (ring Hs of Phe(3), 5H, m); 6.45 (Phe(3) NH, 1H, d, *J*=9 Hz); 6.29 (Val(2) NH, 1H, d, *J*=6 Hz); 4.98 (Tyr(1) NH, 1H, d, *J*=6 Hz); 4.82 (C$^{\alpha}$H of Phe(3), 1H, m);

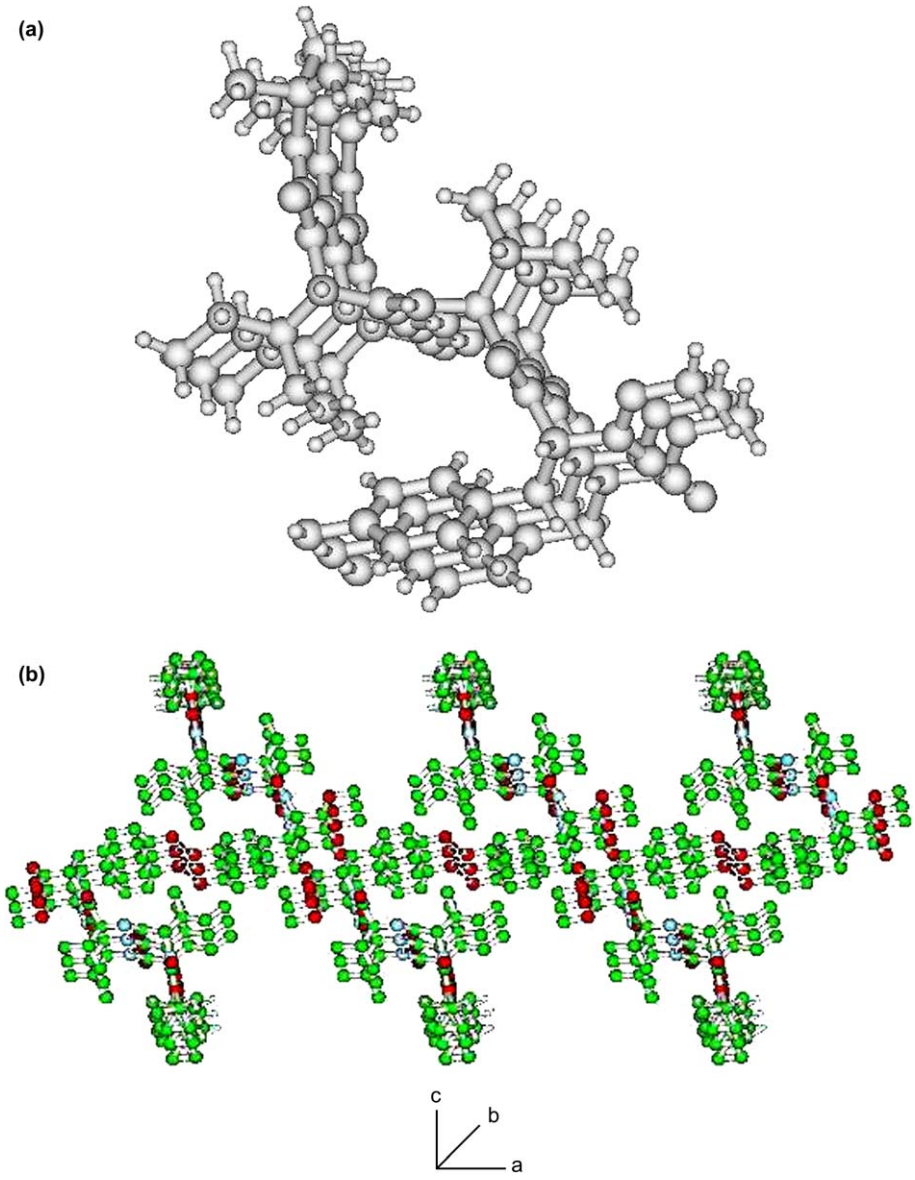

Figure 6. (a) Packing diagram of peptide **5** along crystallographic *b* direction and (b) the crystallographic view of peptide **5** along the axis parallel to the crystallographic *a* axis exhibits that the peptide has failed to form any nanotubular structure, instead it forms quaternary sheet-like structure. Nitrogen atoms are blue, oxygen atoms are red, carbon atoms are green, and hydrogen atoms are gray. Hydrogen bonds are shown as dotted lines.

4.27 ($C^{\alpha}H$ of Val(2), 1H, m); 4.16 ($C^{\alpha}H$ of Tyr(1), 1H, m); 3.70 (–OCH_3, 3H, s); 3.11 ($C^{\beta}Hs$ of Tyr(1), 2H, m); 2.97 ($C^{\beta}Hs$ of Phe(3), 2H, m); 2.05 ($C^{\beta}H$ of Val(2), 1H, m); 1.41 (Boc–CH_3s, 9H, s); 0.88–0.77 ($C^{\gamma}Hs$ of Val(2), 6H, m); (found: C, 64.2; H, 7.1; N, 7.65. $C_{29}H_{39}N_3O_7$ (541) requires C, 64.32; H, 7.21; N, 7.76%); ESI-MS *m*/*z* (%): 542.3 (100) $(M+H)^+$, 543.3 (35) $(M+2H)^+$, M_{calcd}=541.

4.2.9. Boc-Tyr(1)-Val(2)-Leu(3)-OMe 4. Boc-Tyr(1)-Val(2)-OH **9** (1.9 g, 5 mmol) in DMF (10 mL) was cooled in an ice-water bath. H-Leu-OMe was isolated from the corresponding methyl ester hydrochloride (1.81 g, 10 mmol) by neutralization, subsequent extraction with ethyl acetate and concentration to 10 mL, and it was added to the reaction mixture, followed immediately by DCC (1.03 g, 5 mmol) and HOBt (0.675 g, 5 mmol). The reaction mixture was stirred for three days. The reaction mixture was then taken in ethyl acetate (60 mL) and the DCU was filtered off. The organic layer was washed with 2 M HCl (3×50 mL), brine (2×50 mL), 1 M sodium carbonate (3×50 mL), and brine (2×50 mL) and then dried over anhydrous sodium sulfate and evaporated in vacuo to yield peptide **4** as a white solid. Purification was done by silica gel column (100–200 mesh) using 3:1 ethyl acetate/toluene as eluent.

Yield=2.03 g (4 mmol, 80%); R_f=0.58 (25% toluene/ethyl acetate); mp 76–78 °C; IR (KBr): 3322, 1691, 1648, 1517 cm^{-1}; $[\alpha]_D^{20}$ −24.3 (*c* 0.5, CH_3OH); ^1H NMR (300 MHz, $CDCl_3$) δ 7.02 (ring Hs of Tyr(1), 2H, d, *J*=8.4 Hz), 6.75 (ring Hs of Tyr(1), 2H, d, *J*=8.1 Hz); 6.6 (Leu(3) NH, 1H, d, *J*=8.7 Hz); 6.45 (Val(2) NH, 1H, d, *J*=7.5 Hz); 5.0 (Tyr(1) NH, 1H, d, *J*=6 Hz); 4.56 ($C^{\alpha}H$ of Leu(3), 1H, m); 4.29 ($C^{\alpha}H$ of Val(2), 1H, m); 4.22 ($C^{\alpha}H$ of Tyr(1), 1H, m); 3.72 (–OCH_3, 3H, s); 3.00 ($C^{\beta}Hs$ of

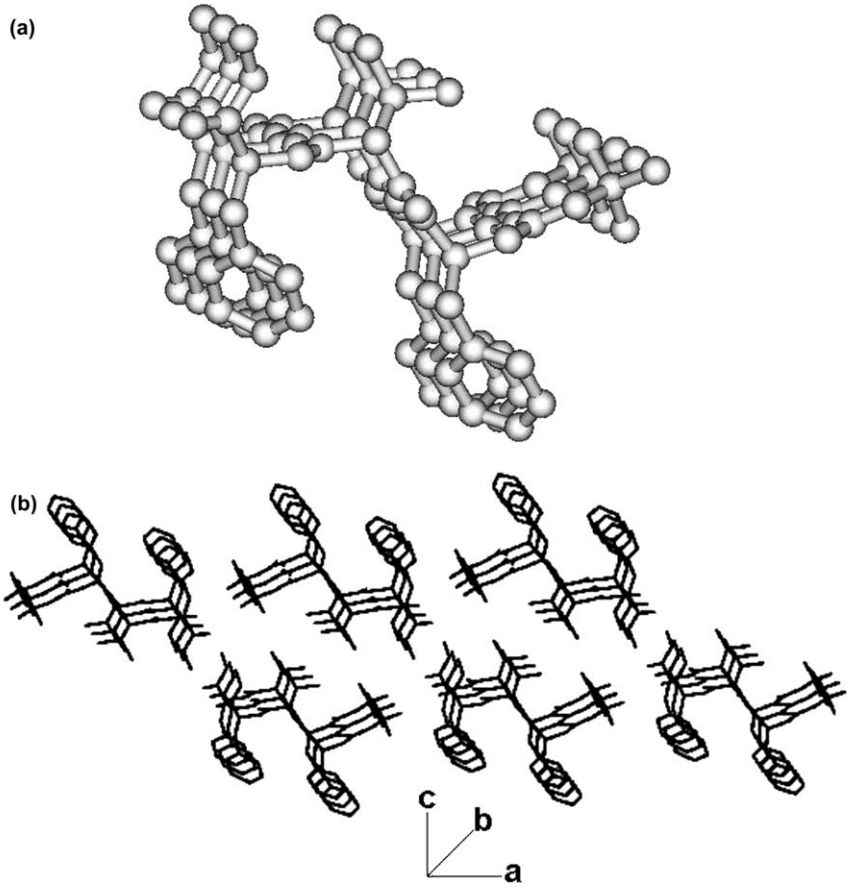

Figure 7. (a) Packing diagram of the peptide **6** showing the formation of intermolecular hydrogen-bonded structure along crystallographic *b* axis and (b) higher order packing of peptide **6**, showing the formation of complex sheet-like structure along *a* axis.

Tyr(1), 2H, m); 2.17–2.03 ($C^{\beta}H$ of Val(2), 1H, m); 1.67–1.58 ($C^{\beta}Hs$ and $C^{\gamma}H$ of Leu(3), 3H, m); 1.41 (Boc–CH_3s, 9H, s); 0.94–0.86 ($C^{\gamma}Hs$ of Val(2) and $C^{\delta}Hs$ of Leu(3), 12H, m); (found: C, 61.2; H, 7.8; N, 8.2. $C_{26}H_{41}N_3O_7$ (507) requires C, 61.54; H, 8.08; N, 8.28%); ESI-MS *m*/*z* (%): 508.4 (100) $(M+H)^+$, M_{calcd}=507.

4.2.10. Boc-Ile(1)-OH 12.[16] A solution of isoleucine (1.31 g, 10 mmol) in a mixture of dioxane (20 mL), water (10 mL), and 1 M NaOH (10 mL) was stirred and cooled in an ice-water bath. Di-*tert*-butylpyrocarbonate (2.2 g, 11 mmol) was added and stirring was continued at room temperature for 6 h. Then the solution was concentrated

Table 3. Crystal and data collection parameters of peptides **3**, **4**, **5**, and **6**

	Peptide **3**	Peptide **4**	Peptide **5**	Peptide **6**
Empirical formula	$C_{29}H_{38}N_3O_7 \cdot 0.5H_2O$	$C_{26}H_{41}N_3O_7$	$C_{26}H_{41}N_3O_7$	$C_{29}H_{39}N_3O_6$
Mol. wt.	1097.25	507.62	507.56	525.63
Data collection	X-Calibur CCD	Image Plate	Image Plate	Image Plate
Radiation, temperature	Cu Kα, 100	Mo Kα, 293	Mo Kα, 293	Mo Kα, 293
Crystallizing solvent	Methanol–water	Methanol–water	Methanol–water	Methanol–water
Crystal system	Monoclinic	Triclinic	Monoclinic	Monoclinic
Space group	*P*2	*P*1	$P2_1$	$P2_1$
a (Å)	22.2063(12)	5.021(7)	16.289(18)	15.327(17)
b (Å)	4.9902(2)	10.435(12)	4.979(7)	5.096(7)
c (Å)	29.0502(12)	14.009(15)	18.931(19)	20.73(2)
α (°)	(90)	80.26(1)	(90)	(90)
β (°)	108.288(4)	87.91(1)	103.57(1)	109.30(1)
γ (°)	(90)	80.23(1)	(90)	(90)
U (Å^3)	3056.6(3)	713(3)	1492(3)	1528(3)
Z	4	1	2	2
Density (calcd, mg/mm^3)	1.192	1.184	1.129	1.142
Unique data	9049	4586	4571	4833
Observed reflections ($I>2\sigma(I)$)	5466	3875	3588	2562
R	0.0465	0.0557	0.1148	0.1018
*wR*2	0.1050	0.1587	0.1931	0.1923
Max, residual e/Å^3	0.264, −0.264	0.193, −0.181	0.245, −0.269	0.283, −0.296

in vacuo to about 15–20 mL, cooled in an ice-water bath, covered with a layer of ethyl acetate (about 30 mL), and acidified with a dilute solution of $KHSO_4$ to pH 2–3 (Congo red). The aqueous phase was extracted with ethyl acetate and this operation was done repeatedly. The ethyl acetate extracts were pooled, washed with water and dried over anhydrous Na_2SO_4, and evaporated in vacuo to obtain **12** as a solid material.

Yield=2.2 g (9.5 mmol, 95%). Elemental Analysis Calcd for $C_{11}H_{21}NO_4$ (231): C, 57.14; H, 9.09; N, 6.06. Found: C, 56.9; H, 8.9; N, 5.9%. Mp 65–67 °C, lit. mp 66–69 °C.

4.2.11. Boc-Ile(1)-Val(2)-OMe 13. Boc-Ile-OH **12** (1.84 g, 8 mmol) was dissolved in dichloromethane (DCM) (10 mL) in an ice-water bath. H-Val-OMe was isolated from the corresponding methyl ester hydrochloride (2.68 g, 10 mmol) by neutralization, subsequent extraction with ethyl acetate and concentration to 10 mL, and it was added to the reaction mixture, followed immediately by di-cyclohexylcarbodiimide (DCC) (1.64 g, 8 mmol). The reaction mixture was allowed to come to room temperature and stirred for 24 h. DCM was evaporated, residue was taken in ethyl acetate (60 mL), and dicyclohexylurea (DCU) was filtered off. The organic layer was washed with 2 M HCl (3×50 mL), brine (2×50 mL), 1 M sodium carbonate (3×50 mL), and brine (2×50 mL) and then dried over anhydrous sodium sulfate, and evaporated in vacuo to yield **13** as a solid compound.

Yield=2.4 g (7 mmol, 87%); R_f=0.65 (ethyl acetate); mp 78–82 °C; $[\alpha]_D^{20}$ −38.8 (*c* 0.69, CH_3OH); ^{1}H NMR (300 MHz, $CDCl_3$) δ 6.35 (Val(2) NH, 1H, d, *J*=7.5 Hz); 5.03 (Ile(1) NH, 1H, d, *J*=6.6 Hz); 4.54 (C^{α}H of Val(2), 1H, m); 3.94 (C^{α}H of Ile(1), 1H, m); 3.73 (–OCH_3, 3H, s); 2.15 (C^{β}H of Val(2), 1H, m); 1.86 (C^{β}H of Ile(1), 1H, m); 1.67–1.62 (C^{γ}Hs of Ile(1), 2H, m); 1.42 (Boc–CH_3s, 9H, s); 0.94–0.89 (C^{γ}Hs of Val(2), C^{γ}Hs and C^{δ}Hs of Ile(1), 12H, m); (found: C, 59.0; H, 8.21; N, 8.03. $C_{17}H_{32}N_2O_5$ (344) requires C, 59.30; H, 9.30; N, 8.14%).

4.2.12. Boc-Ile(1)-Val(2)-OH 14. Boc-Ile(1)-Val(2)-OMe **13** (2.23 g, 6.5 mmol), MeOH (20 mL), and 2 M NaOH (10 mL) were added and the progress of saponification was monitored by thin layer chromatography (TLC). The reaction mixture was stirred. After 10 h methanol was removed under vacuo, the residue was taken in 50 mL of water and washed with diethyl ether (2×50 mL). Then the pH of the aqueous layer was adjusted to 2 using 1 M HCl and it was extracted with ethyl acetate (3×50 mL). The extracts were pooled, dried over anhydrous sodium sulfate, and evaporated in vacuo to yield **14** as a waxy solid.

Yield=1.8 g (5.5 mmol, 84%); ^{1}H NMR (300 MHz, $(CD_3)_2SO$) δ 12.46 (–COOH, 1H, b); 7.70 (Val(2) NH, 1H, d, *J*=6 Hz); 6.69 (Ile(1) NH, 1H, d, *J*=9 Hz); 4.08 (C^{α}H of Val(2), 1H, m); 3.79 (C^{α}H of Ile(1), 1H, m); 2.44 (C^{β}H of Val(2), 1H, m); 1.97 (C^{β}H of Ile(1), 1H, m); 1.60 (C^{γ}Hs of Ile(1), 2H, m); 1.3 (Boc–CH_3s, 9H, s); 1.03–0.96 and 0.82–0.70 (C^{γ}Hs and C^{δ}Hs of Ile(1) and C^{γ}Hs of Val(2), 12H, m); (found: C, 58.01; H, 9.13; N, 8.34. $C_{16}H_{30}N_2O_5$ (330) requires C, 58.18; H, 9.09; N, 8.48%).

4.2.13. Boc-Ile(1)-Val(2)-Tyr(3)-OMe 5. Boc-Ile(1)-Val(2)-OH **14** (1.65 g, 5 mmol) in DMF (10 mL) was cooled in an ice-water bath. H-Tyr-OMe was isolated from the corresponding methyl ester hydrochloride (2.31 g, 10 mmol) by neutralization, subsequent extraction with ethyl acetate and concentration to 10 mL, and it was added to the reaction mixture, followed immediately by DCC (1.03 g, 5 mmol) and HOBt (0.675 g, 5 mmol). The reaction mixture was stirred for three days. The reaction mixture was then taken in ethyl acetate (60 mL) and the DCU was filtered off. The organic layer was washed with 2 M HCl (3×50 mL), brine (2×50 mL), 1 M sodium carbonate (3×50 mL), and brine (2×50 mL) and then dried over anhydrous sodium sulfate and evaporated in vacuo to yield peptide **5** as a white solid. Purification was done by silica gel column (100–200 mesh) using 3:1 ethyl acetate/toluene as eluent.

Yield=2.23 g (4.4 mmol, 89%); R_f=0.64 (25% toluene/ethyl acetate); mp 110–112 °C; IR (KBr): 3488, 3313, 1739, 1692, 1645, 1522 cm^{-1}; $[\alpha]_D^{20}$ −35 (*c* 0.5, CH_3OH); ^{1}H NMR (300 MHz, $CDCl_3$) δ 6.92 (ring Hs of Tyr(3), 2H, d, *J*=9 Hz), 6.74 (ring Hs of Tyr(3), 2H, d, *J*=8.4 Hz); 6.60 (Tyr(3) NH, 1H, d, *J*=8.7 Hz); 6.45 (Val(2) NH, 1H, d, *J*=8.1 Hz); 5.01 (Ile(1) NH, 1H, d, *J*=9 Hz); 4.82 (C^{α}H of Tyr(3), 1H, m); 4.23 (C^{α}H of Val(2), 1H, m); 3.94 (C^{α}H of Ile(1), 1H, m); 3.72 (–OCH_3, 3H, s); 3.10–2.94 (C^{β}Hs of Tyr(3), 2H, m); 2.12–2.05 (C^{β}H of Val(2), 1H, m); 1.95–1.90 (C^{β}H of Ile(1), 1H, m); 1.44 (Boc–CH_3s, 9H, s); 1.28 (C^{γ}Hs of Ile(1), 2H, m); 0.91–0.87 (C^{γ}Hs of Val(2) and C^{γ}Hs and C^{δ}Hs of Ile(1), 12H, m); (found: C, 61.34; H, 8.10; N, 8.06. $C_{26}H_{41}N_3O_7$ (507) requires C, 61.53; H, 8.09; N, 8.28%); ESI-MS *m/z* (%): 508.4 (100) $(M+H)^+$, 509.4 (30) $(M+2H)^+$, M_{calcd}=507.

4.2.14. Boc-Phe(1)-OH 15. See Ref. 17.

4.2.15. Boc-Phe(1)-Val(2)-OMe 16. Boc-Phe-OH (2.65 g, 10 mmol) was dissolved in dichloromethane (DCM) (10 mL) in an ice-water bath. H-Val-OMe was isolated from the corresponding methyl ester hydrochloride (3.34 g, 20 mmol) by neutralization, subsequent extraction with ethyl acetate and concentration to 10 mL, and it was added to the reaction mixture, followed immediately by di-cyclohexylcarbodiimide (DCC) (2.06 g, 10 mmol). The reaction mixture was allowed to come to room temperature and stirred for 24 h. DCM was evaporated, residue was taken in ethyl acetate (60 mL), and dicyclohexylurea (DCU) was filtered off. The organic layer was washed with 2 M HCl (3×50 mL), brine (2×50 mL), 1 M sodium carbonate (3×50 mL), and brine (2×50 mL) and then dried over anhydrous sodium sulfate, and evaporated in vacuo to yield **16** as a white solid.

Yield=3.5 g (9.2 mmol, 92%); R_f=0.76 (ethyl acetate); mp 58–60 °C; ^{1}H NMR (300 MHz, $CDCl_3$) δ 7.32–7.19 (ring Hs of Phe(1), 5H, m); 6.36 (Val(2) NH, 1H, d, *J*=8.4 Hz); 5.01 (Phe(1) NH, 1H, d, *J*=8.1 Hz); 4.45 (C^{α}H of Val(2), 1H, m); 4.35 (C^{α}H of Phe(1), 1H, m); 3.69 (–OCH_3, 3H, s); 3.07 (C^{β}Hs of Phe(1), 2H, d, *J*=6 Hz); 2.13–2.04 (C^{β}H of Val(2), 1H, m); 1.42 (Boc–CH_3s, 9H, s); 0.88–0.83 (C^{γ}Hs of Val(2), 6H, m); (found: C, 63.2; H, 7.6; N, 7.03. $C_{20}H_{30}N_2O_5$ (378) requires C, 63.49; H, 7.94; N, 7.4%).

4.2.16. Boc-Phe(1)-Val(2)-OH 17. Boc-Phe(1)-Val(2)-OMe **16** (2.3 g, 6 mmol), MeOH (20 mL), and 2 M NaOH (10 mL) were added. The reaction mixture was stirred and the progress of saponification was monitored by thin layer chromatography (TLC). After 10 h methanol was removed under vacuo, the residue was taken in 50 mL of water, washed with diethyl ether (2×50 mL). Then the pH of the aqueous layer was adjusted to 2 using 1 M HCl and it was extracted with ethyl acetate (3×50 mL). The extracts were pooled, dried over anhydrous sodium sulfate, and evaporated in vacuo to yield **17** as a white solid sample.

Yield=1.89 g (5.2 mmol, 86.5%); mp 56–58 °C; ^{1}H NMR (300 MHz, $(CD_3)_2SO$) δ 12.57 (–COOH, 1H, b); 7.86 (Val(2) NH, 1H, d, J=8.6 Hz); 7.27–7.19 (ring Hs of Phe(1), 5H, m); 6.95 (Phe(1) NH, 1H, d, J=8.7 Hz); 4.22 (C^{α}H of Val(2), 1H, m); 4.01 (C^{α}H of Phe(1), 1H, m); 2.99–2.93 (C^{β}Hs of Phe(1), 2H, m); 2.77–2.69 (C^{β}H of Val(2), 1H, m); 1.29 (Boc–CH_3s, 9H, s); 1.15–0.81 (C^{γ}Hs of Val, 6H, m); (found: C, 62.45; H, 7.54; N, 7.52. $C_{19}H_{28}N_2O_5$ (364) requires C, 62.63; H, 7.69; N, 7.69%).

4.2.17. Boc-Phe(1)-Val(2)-Phe(3)-OMe 6. Boc-Phe(1)-Val(2)-OH **17** (1.82 g, 5 mmol) in DMF (10 mL) was cooled in an ice-water bath. H-Phe-OMe was isolated from the corresponding methyl ester hydrochloride (2.15 g, 10 mmol) by neutralization, subsequent extraction with ethyl acetate and concentration to 10 mL, and it was added to the reaction mixture, followed immediately by DCC (1.03 g, 5 mmol) and HOBt (0.675 g, 5 mmol). The reaction mixture was stirred for three days. The reaction mixture was taken in ethyl acetate (60 mL) and the DCU was filtered off. The organic layer was washed with 2 M HCl (3×50 mL), brine (2×50 mL), 1 M sodium carbonate (3×50 mL), and brine (2×50 mL) and then dried over anhydrous sodium sulfate and evaporated in vacuo to yield peptide **6** as a white solid. Purification was done by silica gel column (100–200 mesh) using 3:1 ethyl acetate/toluene as eluent.

Yield=2.3 g (4.4 mmol, 87%); R_f=0.70 (25% toluene/ethyl acetate); mp 76–78 °C; IR (KBr): 3329, 3295, 1741, 1691, 1649, 1530 cm^{-1}, $[\alpha]_D^{20}$ −29.4 (c 0.5, CH_3OH); ^{1}H NMR (300 MHz, $CDCl_3$) δ 7.33–7.08 (ring Hs of Phe(1) and Phe(3), 10H, m); 6.47 (Phe(3) NH, 1H, d, J=8.4 Hz); 6.23 (Val(2) NH, 1H, d, J=7.5 Hz); 4.93 (Phe(1) NH, 1H, d, J=8.1 Hz); 4.80 (C^{α}H of Phe(3), 1H, m); 4.35 (C^{α}H of Val(2), 1H, m); 4.16 (C^{α}H of Phe(1), 1H, m); 3.7 (–OCH_3, 3H, s); 3.15–3.02 (C^{β}Hs of Phe(1) and Phe(3), 4H, m); 2.10–2.00 (C^{β}H of Val(2), 1H, m); 1.40 (Boc–CH_3s, 9H, s); 0.81 (C^{γ}Hs of Val(2), 6H, m); (found: C, 61.92; H, 7.31; N, 7.92. $C_{29}H_{39}N_3O_6$ (525) requires C, 66.28; H, 7.42; N, 8.00%); ESI-MS m/z (%): 526.3 (100) $(M+H)^+$, 1073.6 (50) $(2M+H)^+$, M_{calcd}=525.

4.3. Single crystal X-ray diffraction study

Single crystals suitable for X-ray diffraction studies for tripeptides **3**–**6** were grown from methanol–water solution by slow evaporation. Diffraction data were measured for tripeptide **3** with Cu Kα radiation at 100 K using the Oxford Instruments X-Calibur CCD system and for **4**, **5**, and **6** with Mo Kα radiation at 293 K using the MAR research Image Plate System. A crystal of peptide **3** was positioned at 50 mm from the CCD and 330 frames were measured with a counting time of 10 s. Data analysis was carried out with the Crysalis program.[18] For peptides **4**, **5**, and **6**, the crystals were positioned at 70 mm from the Image Plate and 100 frames were measured at 2° intervals with a counting time of 2–5 min for various peptides. Data analyses were carried out with the XDS program.[19] The structures were solved using direct methods with the Shelx97[20] program. All non-hydrogen atoms of all peptides were refined with anisotropic thermal parameters. The hydrogen atoms were included in geometric positions and given thermal parameters equivalent to 1.2 times those of the atom to which they were attached. The structures were refined on F^2 using Shelx97. Crystallographic data for the peptides **3**–**6** have been deposited at the Cambridge Crystallographic Data Centre (CCDC 264909–264911 and 298754).

4.4. ^{1}H NMR experiments

All NMR studies were carried out on a Brüker DPX 300 MHz spectrometer at 300 K. Peptide concentrations were in the range of 1–10 mmol in $CDCl_3$ and $(CD_3)_2SO$.

4.5. Mass spectrometry

Mass spectra were recorded on a Hewlett Packard Series 1100MSD mass spectrometer by positive mode electrospray ionization.

Acknowledgements

We thank EPSRC and the University of Reading, UK for funds for the Oxford Instruments X-Calibur and Marresearch Image Plate Systems. We acknowledge the DST, New Delhi, India for financial assistance Project no. (SR/S5/OC-29/2003). S.R. and A.K. wish to acknowledge the CSIR, New Delhi, India for financial assistance.

References and notes

1. (a) Harada, A.; Li, J.; Kamachi, M. *Nature* **1993**, *346*, 516–518; (b) Nelson, J. C.; Saven, J. G.; Moore, J. S.; Wolynes, P. G. *Science* **1997**, *277*, 1793–1796; (c) Bong, D. T.; Clark, T. D.; Granja, J. R.; Ghadiri, M. R. *Angew. Chem., Int. Ed.* **2001**, *40*, 988–1011; (d) Fenniri, H.; Deng, B.-L.; Ribbe, A. E.; Hallenga, K.; Jacob, J.; Thiyagarajan, P. *Proc. Natl. Acad. Sci. U.S.A.* **2002**, *99*, 6487–6492.
2. (a) Lear, J. D.; Wasserman, Z. R.; Degrado, W. F. *Science* **1988**, *240*, 1177–1181; (b) Ghadiri, M. R.; Granja, J. R.; Milligan, R. A.; McRee, D. E.; Kazanovich, N. *Nature* **1993**, *366*, 324–327; (c) Sakai, N.; Brennan, K. C.; Weiss, L. A.; Matile, S. *J. Am. Chem. Soc.* **1997**, *119*, 8726–8727; (d) Sakai, N.; Majumdar, N.; Matile, S. *J. Am. Chem. Soc.* **1999**, *121*, 4294–4295.
3. Granja, J. R.; Ghadiri, M. R. *J. Am. Chem. Soc.* **1994**, *116*, 10785–10786.
4. Sanchez-Ouesada, J.; Isler, M. P.; Ghadiri, M. R. *J. Am. Chem. Soc.* **2002**, *124*, 10004–10005.
5. (a) Fernandez-Lopez, S.; Kim, H.-S.; Choi, E. C.; Delgado, M.; Granja, J. R.; Khasanov, A.; Kraehenbuehl, K.; Long, G.; Weinberger, D. A.; Wilcoxen, K. M.; Ghadiri, M. R. *Nature*

2001, *412*, 452–455; (b) Hartgerink, J. D.; Granja, J. R.; Milligan, R. A.; Ghadiri, M. R. *J. Am. Chem. Soc.* **1996**, *118*, 43–50; (c) Amorin, M.; Castedo, L.; Granja, J. R. *J. Am. Chem. Soc.* **2003**, *125*, 2844–2845; (d) Rosenthal-Aizman, K.; Svensson, G.; Unden, A. *J. Am. Chem. Soc.* **2004**, *126*, 3372–3373; (e) Horne, W. S.; Ashkenasy, N.; Ghadiri, M. R. *Chem.—Eur. J.* **2005**, *11*, 1137–1144.

6. (a) Gademann, K.; Seebach, D. *Helv. Chim. Acta* **1999**, *82*, 957–962; (b) Seebach, D.; Matthews, J. L.; Meden, A.; Wessels, T.; Baerlocher, C.; McCusker, L. B. *Helv. Chim. Acta* **1997**, *80*, 173–182; (c) Clark, T. D.; Buehler, L. K.; Ghadiri, M. R. *J. Am. Chem. Soc.* **1998**, *120*, 651–656.
7. Karle, I. L.; Handa, B. K.; Hassell, C. H. *Acta Crystallogr.* **1975**, *B31*, 555–560.
8. Gauthier, D.; Baillargeon, P.; Drouin, M.; Dory, Y. L. *Angew. Chem., Int. Ed.* **2001**, *40*, 4635–4638.
9. Semetey, V.; Didierjean, C.; Briand, J.-P.; Aubry, A.; Guichard, G. *Angew. Chem., Int. Ed.* **2002**, *41*, 1895–1898.
10. Kraus, T.; Buděšínský, M.; Císařová, I.; Závada, J. *Angew. Chem., Int. Ed.* **2002**, *41*, 1715–1717.
11. Seela, F.; Wiglenda, T.; Rosemeyer, H.; Eickmeier, H.; Reuter, H. *Angew. Chem., Int. Ed.* **2002**, *41*, 603–604.
12. (a) Fenniri, H.; Mathivanan, P.; Vidale, K. L.; Sherman, D. M.; Hallenga, K.; Wood, K. V.; Stowell, J. G. *J. Am. Chem. Soc.* **2001**, *123*, 3854–3855; (b) Fenniri, H.; Deng, B.-L.; Ribbe, A. E. *J. Am. Chem. Soc.* **2002**, *124*, 11064–11072; (c) Moralez, G. J.; Raez, J.; Yamazaki, T.; Motkuri, K. R.; Kovalenko, A.; Fenniri, H. *J. Am. Chem. Soc.* **2005**, *127*, 8307–8309.
13. (a) Görbitz, C. H. *Chem.—Eur. J.* **2001**, *7*, 5153–5159; (b) Reches, M.; Gazit, E. *Science* **2003**, *300*, 625–627; (c) Song, Y.; Challa, S. R.; Medforth, C. J.; Qiu, Y.; Watt, R. K.; Peňa, D.; Miller, J. E.; Swol, F. v.; Shelnutt, J. A. *Chem. Commun.* **2004**, 1044–1045; (d) Lu, K.; Jacob, J.; Thiyagarajan, P.; Conticello, V. P.; Lynn, D. G. *J. Am. Chem. Soc.* **2003**, *125*, 6391–6393; (e) Vauthey, S.; Santoso, S.; Gong, H.; Watson, N.; Zhang, S. *Proc. Natl. Acad. Sci. U.S.A.* **2002**, *99*, 5355–5360; (f) Ray, S.; Haldar, D.; Drew, M. G. B.; Banerjee, A. *Org. Lett.* **2004**, *6*, 4463–4465.
14. Ramachandran, G. N.; Sasisekharan, V. *Adv. Protein Chem.* **1968**, *23*, 284–438.
15. Bodanszky, M.; Bodanszky, A. *The Practice of Peptide Synthesis*; Springer: New York, NY, 1984; pp 1–282.
16. Keller, O.; Keller, W. E.; van Look, G.; Wersin, G. *Organic Syntheses*; Wiley & Sons: New York, NY, 1990; Collect. Vol. VII, p 70.
17. Das, A. K.; Banerjee, A.; Drew, M. G. B.; Ray, S.; Haldar, D.; Banerjee, A. *Tetrahedron* **2005**, *61*, 5027–5036.
18. Crysalis Version 1; Oxford Instruments: 2005.
19. Kabsch, W. *J. Appl. Crystallogr.* **1988**, *21*, 916–924.
20. Sheldrick, G. M. *Shelx97, Program for Crystal Structure Refinement*; University of Gottingen: 1997.